the hydrophobicity of the amphiphile and that the number of exposed hydrophobic residues is an important determinant in the mechanism of lipid–protein association. This hypothesis, however, requires a more rigorous test.

Acknowledgments

We thank Sarah Myers and Sharon Bonnot for their assistance in the preparation of the manuscript and Susan McNeely for providing the line drawings. The technical assistance of Leonore Pownall is also gratefully acknowledged.

References

Assmann, G., & Brewer, H. B., Jr. (1974) *Proc. Natl. Acad. Sci. U.S.A. 71*, 989–993.
Blok, M. C., van der Neut-kok, E. C. M., van Deenen, L. L. M., & de Gier, J. (1975) *Biochim. Biophys. Acta 406*, 187.
Brown, W. V., Levy, R. I., & Fredrickson, D. S. (1969) *J. Biol. Chem. 244*, 5687–5694.
Charlton, S. C., Olson, J. S., Hong, K.-Y., Pownall, H. J., Louis, D. D., & Smith, L. C. (1976), *J. Biol. Chem. 251*, 7952–7955.
Doody, M. C., Pownall, H. J., Kao, Y. J., & Smith, L. C. (1980) *Biochemistry 19*, 108.
Harlos, K., Vaz, W. L. C., & Kovatchev, S. (1977) *FEBS Lett. 77*, 7.
Jackson, R. L., Morrisett, J. D., Pownall, H. J., & Gotto, A. M., Jr. (1973) *J. Biol. Chem. 248*, 5218–5224.
Jackson, R. L., Morrisett, J. D., & Gotto, A. M. (1976) *Physiol. Rev. 56*, 259.
Jonas, A., & Krajnovich, D. J. (1977) *J. Biol. Chem. 252*, 2194.
Kanehisa, M. I., & Tsong, T. Y. (1978) *J. Am. Chem. Soc. 100*, 424.
Leto, T. L., Roseman, M. A., & Holloway, P. W. (1980) *Biochemistry 19*, 1911.
Marsh, D., Watts, A., & Knowles, P. F. (1976) *Biochemistry 15*, 3570.
op den Kamp, J. A. F., Kauerz, M. T., & van Deenen, L. L. M. (1975) *Biochim. Biophys. Acta 406*, 169.
Osborne, J. C., & Brewer, H. B. (1977) *Adv. Protein Chem. 31*, 253.
Osborne, J. C., Palumbo, G., Brewer, H. B., & Edelhoch, H. (1975) *Biochemistry 14*, 3741.
Papahadjopoulas, D., Jacobson, K., Nir, S., & Isac, T. (1973) *Biochim. Biophys. Acta 311*, 330.
Patel, K., & Sparrow, J. T. (1978) *J. Chromatogr. 150*, 542.
Patel, K., Morrisett, J. D., & Sparrow, J. T. (1979) *J. Lipid Res. 20*, 674.
Pownall, H. J., Massey, J. B., Kusserow, S. K., & Gotto, A. M., Jr. (1978a) *Biochemistry 17*, 1183.
Pownall, H. J., Pao, Q., Rohde, M., & Gotto, A. M., Jr. (1978b) *Biochem. Biophys. Res. Commun. 85*, 408.
Pownall, H. J., Massey, J. B., Kusserow, S. K., & Gotto, A. M., Jr. (1979) *Biochemistry 18*, 574.
Pownall, H. J., Hu, A., Albers, J. J., Gotto, A. M., & Sparrow, J. T. (1980) *Proc. Natl. Acad. Sci. U.S.A. 77*, 3154.
Reynolds, J. A. (1976) *J. Biol. Chem. 251*, 6013.
Reynolds, J. A., Tanford, C., & Stone, W. L. (1977) *Proc. Natl. Acad. Sci. U.S.A. 74*, 3796–3799.
Roseman, M. A., & Thompson, T. E. (1980) *Biochemistry 19*, 439–444.
Smith, L. C., Pownall, H. J., & Gotto, A. M. (1978) *Annu. Rev. Biochem. 47*, 751.
Sparrow, J. T. (1976) *J. Org. Chem. 41*, 1350–1353.
Sparrow, J. T., Pownall, H. J., Sigler, G. F., Smith, L. C., Soutar, A. K., & Gotto, A. M., Jr. (1977) *Pept., Proc. Am. Pept. Symp., 5th*, 149.
Swaney, J. B. (1980) *J. Biol. Chem. 255*, 8791.
Tall, A., Shipley, G. G., & Small, D. M. (1976) *J. Biol. Chem. 251*, 3749.
Tsong, T. Y. (1975) *Biochemistry 14*, 5409.
Wu, S. H., & McConnell, H. M. (1973) *Biochem. Biophys. Res. Commun. 55*, 484.

Phase Equilibria in Binary Mixtures of Dimyristoylphosphatidylcholine and Cardiolipin†

Theo Berclaz‡ and Harden M. McConnell*

ABSTRACT: Paramagnetic resonance spectra of the spin-label 2,2,6,6-tetramethylpiperidinyl-1-oxy have been used to study phase separations in binary mixtures of dimyristoylphosphatidylcholine and cardiolipin. Two different samples of cardiolipin were used: (i) One sample contained calcium ions at a mole ratio of calcium:cardiolipin = 1:2; the experimental data support the view that cardiolipin is present in the bilayer membrane as calcium ion linked dimers, $(CL)_2Ca^{2+}$. (ii) A calcium-free sodium cardiolipin sample yielded remarkable spin-label partition data that were quite different from those obtained in the presence of Ca^{2+}. In both cases the spin-label data provide evidence for compound formation and for fluid–fluid immiscibility in the bilayer membrane.

There have been numerous studies of the physical properties of binary mixtures of lipids. In a number of cases phase diagrams describing lateral phase separations in planar bilayer membranes have been described [see, e.g., Shimshick & McConnell (1973), Grant et al. (1974), Luna & McConnell (1977), Gent & Ho (1978), Lentz et al. (1978), Mabrey et al. (1978), Oldfield & Chapman (1972), and Ladbrooke & Chapman (1969)]. The most common type of two-phase equilibria that has been encountered is that in which the temperatures and compositions are such that a "solid" phase is in equilibrium with a "fluid" phase. For the purposes of the present paper, we consider a fluid lipid bilayer to be one

† From the Stauffer Laboratory for Physical Chemistry, Stanford University, Stanford, California 94305. *Received March 31, 1981.* This research was supported by National Science Foundation Grant PCM 77-23586 and The Alexander Medical Foundation. The Swiss Fonds National de la Recherche and Stiftung für Stipendien auf dem Gebiete der Chemie are gratefully acknowledged for financial support to T.B.

‡ Present address: Université de Genève, Dept. Chimie-Phys., CH-1211 Genève 4, Switzerland.

0006-2960/81/0420-6635$01.25/0

in which the lateral diffusion coefficients of the lipid molecules are large ($D \simeq 10^{-7}$–10^{-8} cm^2/s) and the solid phases to be those in which the lateral diffusion coefficients are small ($D \leq 10^{-10}$ cm^2/s). Although such phase equilibria may be significant for the structure and function of some biological membranes, it does appear likely that the membranes of most eukaryotic cells are largely fluid, at least as far as lipid diffusion is concerned. This conclusion nonetheless leaves open the question as to whether or not there exist phase separations in the fluid state of bilayer membranes, i.e., "fluid–fluid immiscibility". Such phase separations might easily escape detection with calorimetric, freeze–fracture electron microscopic, or spectroscopic techniques. For a discussion of this problem, and references to earlier work, see Melchior & Steim (1979).

Spin-labels have been previously used to obtain evidence suggesting fluid–fluid immiscibility in binary mixtures of lipids (Wu & McConnell, 1975; Galla & Sackmann, 1975; Rubenstein et al., 1980; Recktenwald & McConnell, 1981). In the present work we have studied the partitioning of the spin-label 2,2,6,6-tetramethylpiperidinyl-1-oxy (Tempo)[1] between water and binary mixtures of dimyristoylphosphatidylcholine (DMPC) and cardiolipin (CL), in both the presence and absence of calcium ion. From the present work we reach the conclusion that there are phase separations involving fluid phases in these binary mixtures of phospholipids.

Materials and Methods

DMPC, Grade A, was purchased from Calbiochem (La Jolla, CA) and stored as 2 and 17 mM stock solutions in either MeOH or EtOH under argon. Cardiolipin from bovine heart was purchased from two different suppliers: (a) from Supelco, Inc. (Bellefonte, PA), as 50 mg/mL in $CHCl_3$, stored and used after dilution to 2 mM in $CHCl_3$ under argon (atomic absorption spectrophotometry showed this CL contained 1 molecule of calcium/2 molecules of CL), and (b) from Sigma Chemical Co. (St. Louis, MO), as 3.34 mg/mL in EtOH, supplied as the sodium salt (atomic absorption spectrophotometry did not detect any calcium in such samples). The fluorescent lipid probe *N*-(7-nitro-2,1,3-benzoxadiazol-4-yl)-phosphatidylethanolamine (NBD-PE) was purchased from Avanti Biochemicals (Birmingham, AL) as 1 mg/mL in hexane–ethanol (9:1). All lipids were used without further purification. Tempo was used at about 10^{-4} M in phosphate-buffered saline (PBS) solution containing 1 mM ethylenediaminetetraacetic acid (EDTA).

Sample Preparation. For the measurement of Tempo partitioning, 5 mg of total lipid of appropriate composition in DMPC and cardiolipin was dried to a film from the stock solution in alcohol, then redissolved into a mixture of $CHCl_3$–MeOH (10:1), and finally dried to a film under reduced pressure. Returning to normal pressure was always done by introducing argon into the flask. Then the film was hydrated at 45 °C for 5 min with 160 μL of Tempo in PBS/EDTA solution, and the well-hydrated lipids were vortexed for several seconds. The liposome suspension was allowed to rest for a few seconds before 50 μL was taken and introduced into a capillary tube which was immediately sealed. EPR spectra were taken as previously described (Rubenstein et al., 1980). Tempo partitioning into phospholipid–cardiolipin liposomes was measured by monitoring the resolved high-field EPR signals for the spin-label dissolved in the hydrophobic (H) and polar (P) environments. The partition coefficient β is equal to the ratio H/P of these two signals. For the diffusion measurements, NBD-PE was added to the original 5 mg of lipids at 0.05 mol %. The liposomes were usually washed once with Tempo solution and resuspended in appropriate amounts of solution before the measurements. The latter were also performed on multibilayers prepared by the procedure already described (Rubenstein et al., 1979). Lateral diffusion measurements were made by using the laser fluorescence photobleaching recovery technique (Smith et al., 1979).

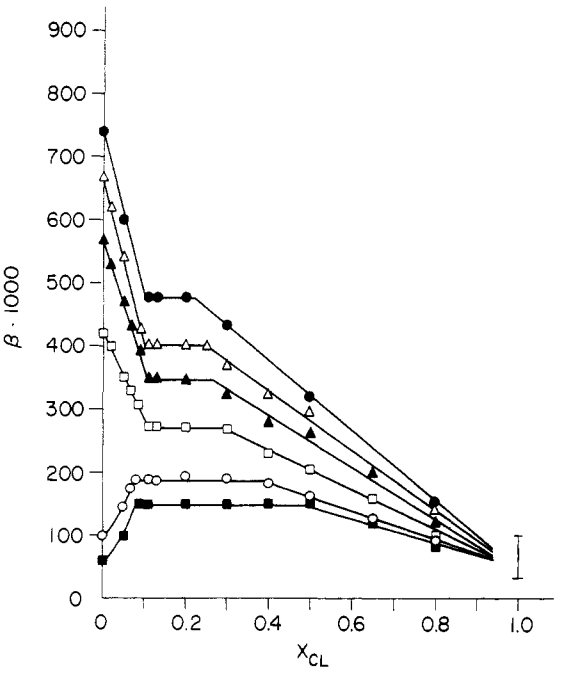

FIGURE 1: Tempo partitioning (β) into DMPC–cardiolipin liposomes as a function of the mole fraction of cardiolipin (X_{CL}) for the calcium–cardiolipin sample (see Materials andd Methods) at (■) 16, (○) 18, (□) 24, (▲) 28, (△) 32, and (●) 40 °C. For X_{CL} = 1.0 (pure cardiolipin), the bar (I) represents the range of β between 16 and 40 °C.

Results

Figure 1 shows the Tempo partition coefficient β as a function of the mole fraction of CL in binary mixtures containing DMPC. These data refer to the "Ca^{2+} sample" (see Materials and Methods). As explained under Discussion we have found it impossible to account for the data in Figure 1 in terms of simple phase equilibria with phases composed of pure DMPC, DMPC plus CL, and pure CL. On the other hand, if CL is assumed to be present in the membranes as a specific complex, $(CL)_2Ca^{2+}$, and the data are plotted as a function of the mole fraction of $(CL)_2Ca^{2+}$, the results (given in Figure 2) are readily understood in terms of such phase equilibria (see Discussion).

The data shown in Figures 1–3 are quite reproducible and show no hysteresis, with the possible exception of the higher temperature and higher CL concentrations ($X_{CL} \lesssim 0.8$, 20–40 °C) in Figure 3 where some lack of reproducibility was noted. The steepness of the peaks may be responsible, in that small errors (e.g., ~1%) in sample composition can produce large errors in β. That is the reason why we did not connect the experimental points for $X_{CL} > 0.80$ in Figure 3, in contrast to what was done for X_{CL} between 0 and 0.80. At other CL compositions and temperatures the maximum errors (based

[1] Abbreviations used: DMPC, dimyristoylphosphatidylcholine; CL, cardiolipin; EDTA, ethylenediaminetetraacetic acid; PBS, phosphate-buffered saline, pH 7.2; Tempo, 2,2,6,6-tetramethylpiperidinyl-1-oxy; NBD-PE, *N*-(7-nitro-2,1,3-benzoxadiazol-4-yl)phosphatidylethanolamine; diI, bis(2-*N*-octadecyl-3,3-dimethyl-1-benz[*b*]pyrrole)trimethincyanine iodide; EPR, electron paramagnetic resonance.

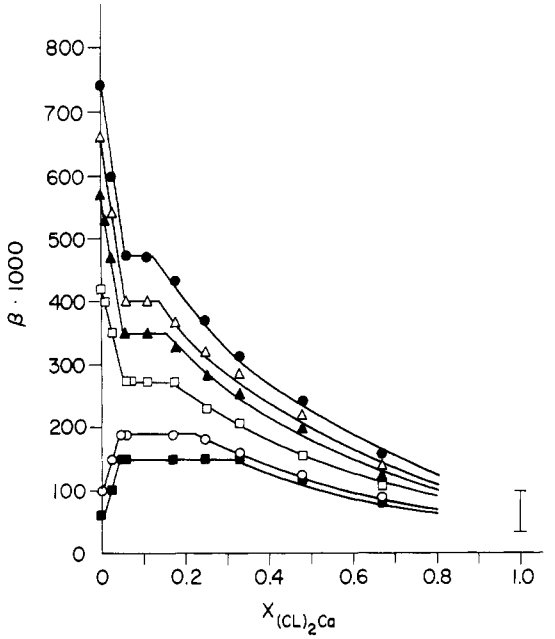

FIGURE 2: Plot of the same Tempo partitioning (β) values as in Figure 1 but as a function of the mole fraction of the calcium-bridged dimer $(CL)_2Ca^{2+}$ at (■) 16, (○) 18, (□) 24, (▲) 28, (△) 32, and (●) 40 °C. For $X_{CL} = 1.0$ (pure cardiolipin), the bar (I) represents the range of β between 16 and 40 °C. The lines represent calculated values based on the model discussed under Appendix. In this figure a number of experimental points have been omitted to prevent overcrowding.

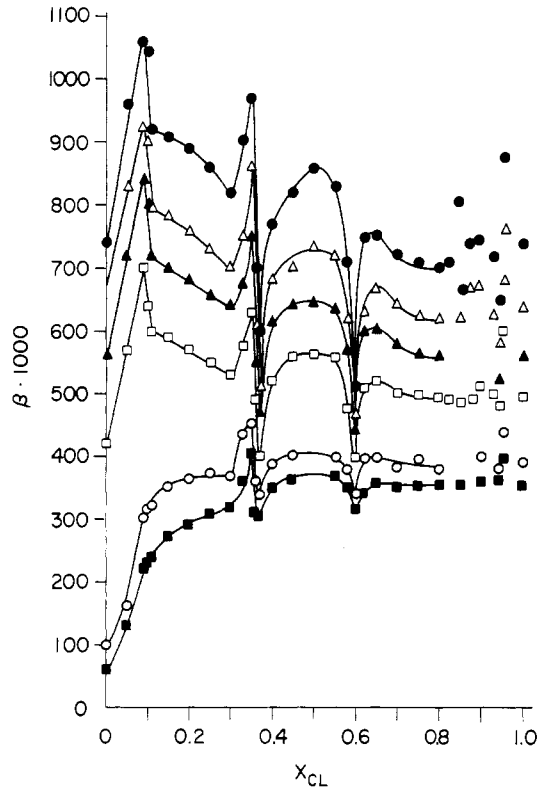

FIGURE 3: Tempo partitioning (β) into DMPC–cardiolipin liposomes expressed as a function of the mole fraction of cardiolipin (X_{CL}) for the calcium-free cardiolipin sample at (■) 16, (○) 18, (□) 24, (▲) 28, (△) 32, and (●) 40 °C. Due to the lack of reproducibility of values for $X_{CL} > 0.8$ the experimental points for this region are not connected with one another as done for $0 < X_{CL} < 0.80$, where experimental data were reproducible. Some of the points for $X_{CL} > 0.8$ can be connected to give curves similar to those in the center of the figure, in the range $0.37 < X_{CL} < 0.60$.

on the reproducibility and self-consistency of the data) are of the order of ±3%.

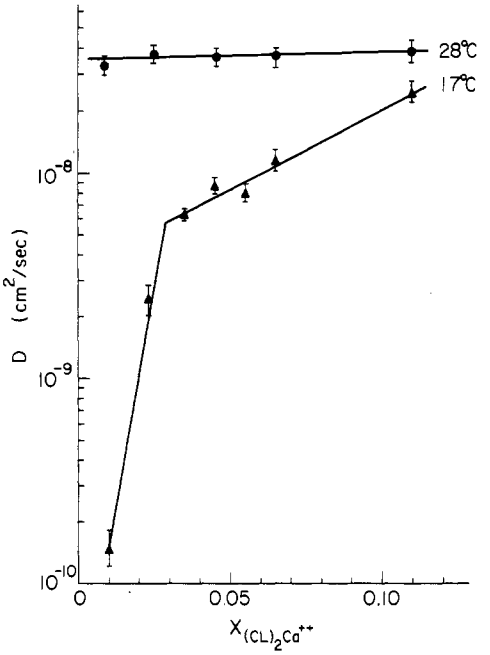

FIGURE 4: Diffusion of the fluorescent lipid probe NBD-PE in DMPC–cardiolipin liposomes as a function of the mole fraction of the calcium-bridged dimer $(CL)_2Ca^{2+}$ at 17 (▲) and 27 °C (●). The bars (I) represent the two extremes of at least four different measurements.

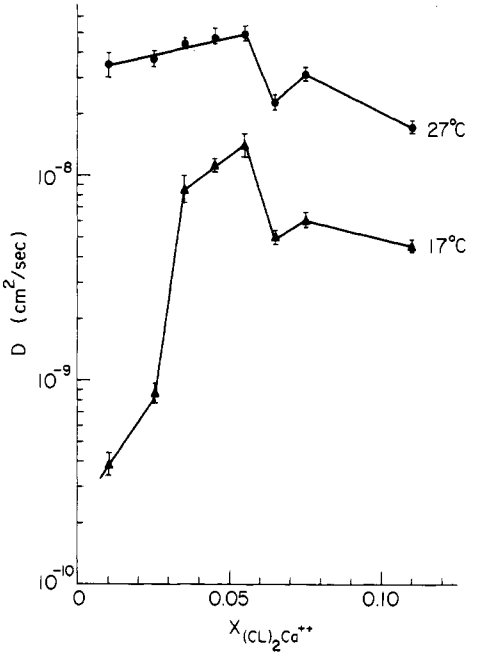

FIGURE 5: Diffusion of the fluorescent lipid probe NBD-PE in DMPC–cardiolipin multibilayers as a function of the mole fraction of the calcium-bridged dimer $(CL)_2Ca^{2+}$ at 17 (▲) and 28 °C (●). The bars (I) represent the two extremes of at least three different measurements.

In all of the Tempo paramagnetic resonance spectra, the hydrophobic and polar signals are well resolved and have no apparent change in line shape, or separation, *except* for spectra taken at the two compositions near the sharp minima in β near $X_{CL} = 0.37$ and $X_{CL} = 0.60$ in Figure 3. At these particular compositions the hydrophobic and polar signals merge somewhat, suggesting an enhanced rate of exchange between Tempo in the hydrophobic and polar phases.

Results of some studies of lateral diffusion in the Ca^{2+} samples are given in Figures 4 and 5 for liposomes and multibilayers. The lateral diffusion coefficients of a fluorescent

lipid probe (NBD-PE) in binary mixtures of DMPC and the Ca^{2+}-containing CL seen in Figures 4 and 5 are quite reminiscent of those observed earlier in binary mixtures of DMPC and cholesterol (Rubenstein et al., 1979). A single measurement of the lateral diffusion of NBD-PE in a Ca^{2+}-free $X_{CL} = 0.50$ binary mixture of CL and DMPC was made, with the result $D \simeq 3.5 \times 10^{-8}$ at 27 °C and 1.7×10^{-8} cm^2/s at 17 °C. The Ca^{2+}-free samples with $X_{CL} = 0.50$ form especially large liposomes, typically 20 μm in diameter. All other lipid samples, both with and without Ca^{2+}, had the appearance of typical liposomes in the optical microscope, except possibly for the Ca^{2+}-containing samples at high CL mole fractions, where the liposomes (sometimes fluorescently labeled) appeared unusually small (less than 1 μm). Preliminary freeze–fracture studies of these samples are in progress in this laboratory; a survey of the Ca^{2+}-containing membranes showed only very few "lipidic structures" of the type discussed by Verkleij et al. (1979) and by Miller (1980). Some diffusion measurements were carried out with the Ca^{2+} samples on multibilayers with the fluorescent lipid probe bis(2-*N*-octadecyl-3,3-dimethyl-1-benzo[*b*]pyrrole)trimethincyanine iodide (diI). These diffusion coefficients were very nearly the same as those reported in Figure 5 for mole fractions of $(CL)_2Ca^{2+}$ between 0.025 and 0.11, at 17 °C.

All the data in Figures 1–4 were obtained for liposomes prepared in PBS, pH 7.0. Other experiments were carried out with the Ca^{2+} samples in distilled water and gave the same shape Tempo partition curves, the main difference being a smaller "salting out effect"; i.e., Tempo binding to a hydrocarbon phase is enhanced when salts are added to the aqueous phase. (This effect is easily demonstrated with mixtures of hexane and water.) The diffusion data given in Figure 5 for multibilayers were obtained with distilled water.

Discussion

In the present work we have encountered two phenomena not previously observed in earlier studies of phase equilibria in binary mixtures of lipids. Consider the Tempo partition data in Figure 1. These β vs. X_{CL} data can clearly be broken up into three regions. In region I, at low CL mole fractions ($X_{CL} < 0.1$), β decreases rapidly with increasing X_{CL}. In the intermediate region, region II, β is remarkably independent of X_{CL}, and in region III β again decreases with increasing X_{CL}. Note that β is essentially a thermodynamic property of the system. Thus the discontinuities in $d\beta/dx$ that mark the boundaries between regions I and II, and regions II and III, must be phase boundaries. According to the phase rule, such boundaries separate one- and two-phase regions for binary mixtures of lipids in systems where the aqueous solvent is in excess. Thus, regions I and III are two-phase regions, and region II is a one-phase region, or vice versa. It is extremely difficult to imagine that region II is a two-phase region, since this would require the two immiscible phases to have identical partition cofficients β. From these arguments alone we conclude that region II must be a one-phase region. In agreement with this assignment it may be noted that the marked similarity between diffusion data in Figures 4 and 5, and diffusion data for binary mixtures of DMPC and cholesterol, strongly indicates that the region $0 \lesssim X_{CL} < 0.1$ at temperatures less than 22 °C is a two-phase region. [For a summary of the studies of the relation between diffusion data and phase equilibria in the DMPC–cholesterol system, see Owicki & McConnell (1980).] This again indicates that region II is a one-phase region. Thus, there is every reason to believe that region I is two phase, region II is one phase, and region III is two phase. The constancy of Tempo partitioning into the one-phase region II is plausible in that all the samples employed had the same total weight and changes in composition within a single homogeneous phase of constant total weight need not give major changes in Tempo binding.

In two-phase regions, the "lever rule" for the construction of phase diagrams places quantitative restrictions on the possible variations of the partition coefficient with composition. As discussed under Appendix, the observed dependence of β on X_{CL} in region III of Figure 1 is not in accord with the assumptions that this is a two-phase region, that the two components are DMPC and CL, and that the lever rule applies. On the other hand, if it is assumed that the CL molecules in this system are present as calcium ion linked dimers, $(CL)_2Ca^{2+}$, and the data replotted as a function of the mole fraction of $(CL)_2Ca^{2+}$ in the sample, then the application of the lever rule fits the data to well within the experimental errors, as can be seen in Figure 2.

The Tempo partition data seen in Figure 3 are certainly the most unusual yet reported for any binary mixture of phospholipids. The compositions corresponding to the various maxima and minima in the Tempo partition parameter β do not change with temperature, within the studied temperature range (except for the maximum at $X_{CL} = 0.09$, which disappears below the chain melting transition temperature of DMPC, 22 °C). We suggest that the compositions corresponding to the sharp maxima (and/or minima) in Tempo partition represent stoichiometric compositions corresponding to "compounds". For example, the maximum at $X_{CL} = 0.50$ in Figure 3 may be an example of compound formation. One may consider two limiting definitions of the word "compound". One can imagine specific clustering of comparatively small groups of molecules within a bilayer membrane, these groups forming well-defined complexes; the bilayer is then considered as some mixture of such complexes. The other limiting view of the word "compound" is that it represents a single thermodynamic phase. We prefer this second interpretation (for the data in Figure 3) even though it raises a second problem. A single homogeneous phase with a simple stoichiometric composition (e.g., $X_{CL} = 0.50$) is expected to have a crystal-like lateral ordering. However, this supposed lateral ordering must nonetheless be consistent with rapid lateral diffusion. Since a number of substances can exhibit both crystal-like order and rapid lateral diffusion (e.g., metallic sodium), our observed rapid lateral diffusion certainly does not rule out this possible crystal-like ordering in CL–DMPC binary mixtures. Assuming crystal-like ordering it is still not possible to say whether the sharp maxima or sharp minima represent such specific compounds. Note that eutectics often have simple stoichiometric compositions (Chadwick, 1963–1964). Also recall that a solid crystalline phase of DMPC (the $P_{\beta'}$ phase) binds Tempo better than a fluid phase mixture of 20 mol % cholesterol and 80 mol % DMPC at the same temperature. Just the opposite result is obtained when $(CL)_2Ca^{2+}$ or CL itself is mixed into the solid $P_{\beta'}$ phase of DMPC; then, the binding of Tempo increases (Figures 2 and 3). In other words, there is no simple monotonic relation between Tempo binding and fluidity (as measured by lateral diffusion, for example).

The data in Figure 2 for binary mixtures of DMPC and $(CL)_2Ca^{2+}$ are also consistent with compound formation, the mole fraction of $(CL)_2Ca^{2+}$ in the compound being of the order of magnitude of 0.1. Thus, each of the curves in Figure 2 corresponds to a different temperature; one can then make a temperature–composition plot by using the points of slope discontinuity given in Figure 2. The resulting curve defines a temperature–composition region in which there is some

miscibility of this putative compound with DMPC and/or $(CL)_2Ca^{2+}$. With this interpretation in mind, examination of the data in Figure 2 leads to the conclusion that this compound becomes unstable at temperatures much above 40 °C. This is in contrast to the data in Figure 3 where there is no indication that the various compounds become unstable at the higher temperatures employed in the present study.

If there is lateral order in the binary mixtures of CL and DMPC, we think it likely that coulombic interactions between the charged CL molecules (together with counterions) play a large role in stabilizing this orrder. The importance of counterions in the formation of ordered distributions of electrically charged solutes in (three-dimensional) aqueous solutions has been emphasized by Ise & Okubo (1980). The closest analogy between earlier studies and the present work may be the "acid soaps". These are compounds of simple stoichiometry formed between fatty acids and their sodium salts. A number of these acid-soap compounds form lamellar phases (Eckwall, 1975).

Until more information about these systems is obtained it is premature to attempt to account for the data in Figure 3 in terms of speculative phase diagrams. It is plausible that the spin-label partition data can be accounted for in terms of phase diagrams involving compounds and eutectics, providing appropriate assumptions are made concerning the relative binding of Tempo to these various phases.

Irrespective of the detailed interpretation of the Tempo partition data in Figures 1–3, we must conclude that immiscible fluid lipid phases are present in these binary lamellar lipid mixtures.

Acknowledgments

We are indebted to Dr. Michael McCloskey for carrying out the freeze–fracture studies mentioned under Results and to Professor David Deamer for bringing the literature on acid soaps to our attention.

Appendix

In all the Tempo partition experiments carried out in the present work, the total weight of lipid was kept constant (5 mg) as was the total weight of water (160 mg). Thus, if we have a two-phase system, one containing pure DMPC and one containing a mixture of DMPC and CL, the observed Tempo partition coefficient β is expected to be related to the Tempo partition coefficients in the two phases, β(DMPC) and β-(DMPC–CL), as follows:

$$\beta = (1/w) \times [w(\text{DMPC})\beta(\text{DMPC}) + w(\text{DMPC–CL})\beta(\text{DMPC–CL})] \quad \text{(A1)}$$

Here w is the total weight of the lipid sample, w(DMPC) is the weight of the DMPC phase, and w(DMPC–CL) is the weight of the phase containing DMPC and CL. We now consider the problem of calculating β as a function of X_{CL}. To do this, it will be convenient to state the problem somewhat more generally.

Assume that we have a binary system with components A and B in which two phases coexist, i and j. If $f^{(i)}$ is the fraction of all the molecules in the sample that are in phase i, then from the well-known lever rule for the construction of phase diagrams

$$f^{(i)} = (X_B^{(j)} - X_B)/(X_B^{(j)} - X_B^{(i)}) \quad \text{(A2)}$$

where $X_B^{(i)}$ and $X_B^{(j)}$ are the mole fractions of B in phases i and j; X_B is the mole fraction of B in the sample. The fraction of all the A molecules in the sample that are in the phase i is $X_A^{(i)}f^{(i)}$, and the fraction of all the B molecules in the sample that are in phase j is $X_B^{(j)}f^{(j)}$. The relative weights of phases i and j are then proportional to

$$w(\text{i}) = M_{r(A)}X_A^{(i)}f^{(i)} + M_{r(B)}X_B^{(i)}f^{(i)} \quad \text{(A3)}$$

$$w(\text{j}) = M_{r(A)}X_A^{(j)}f^{(j)} + M_{r(B)}X_B^{(j)}f^{(j)} \quad \text{(A4)}$$

where $M_{r(A)}$ and $M_{r(B)}$ are the molecular weights of A and B. The total weight of the sample is simply

$$w = w(\text{i}) + w(\text{j}) \quad \text{(A5)}$$

By examination of eq A2–A5 it is clear that the weight fractions $w(\text{i})/w$ and $w(\text{j})/w$ are not in general linear functions of X_B, since X_B appears in both the numerators and denominators of these fractions. Thus, if we identify X_B with X_{CL}, then eq A1 leads to a nonlinear dependence of β on X_{CL}. However, in region I of Figure 1 (see Discussion) the values of X_{CL} are so small ($0 \lesssim X_{CL} \lesssim 0.11$) that the deviations from linearity in caculated β vs. X_{CL} plots are much smaller than the experimental error. An equation analogous to eq A1 also applies to the two-phase temperature composition region of Figure 1, designated III under Discussion.

$$\beta = (1/w)[w(\text{DMPC–CL})\beta(\text{DMPC–CL}) + w(\text{CL})\beta(\text{CL})] \quad \text{(A6)}$$

Here the presumed two coexisting phases are a solution containing a mixture of DMPC and CL and containing pure CL. Again one can attempt to fit the observed data in Figure 2 with eq A2–A5, but in this case calculated β vs. X_{CL} curves show deviations from linearity that are in marked contrast to the linear β vs. X_{CL} lines seen in region III of Figure 1.

As indicated under Discussion, the observed Tempo partition data can be accounted for when it is assumed that CL is a dimeric molecule bound to calcium ion, $(CL)_2Ca^{2+}$. With this assumption eq A6 is modified as follows:

$$\beta = (1/w)[w(\text{DMPC–}(CL)_2Ca^{2+})\beta(\text{DMPC–}(CL)_2Ca^{2+}) + w((CL)_2Ca^{2+})\beta((CL)_2Ca^{2+})] \quad \text{(A7)}$$

When the experimental values of β are plotted vs. the mole fraction of $(CL)_2Ca^{2+}$ in the sample, then eq A2–A5 and eq A7 provide an essentially perfect fit to the experimental data, as seen by comparing the experimental points and calculated curves in Figure 2. Of course, the only a priori "prediction" of the theory is a curvature of the β vs. $X_{(CL)_2Ca^{2+}}$ data on the right-hand side of Figure 2; the end points of these curves are set by the experimental values of β for $X_{(CL)_2Ca^{2+}} = 1$ and the values of β for $X_{(CL)_2Ca^{2+}}$ in the range 0.15–0.35 where the β vs. $X_{(CL)_2Ca^{2+}}$ curves show discontinuities in their slopes. It should be noted that the general thermodynamic reasoning presented here does not require that any of the phases be lamellar and/or part of the same vesicle membrane. All of the phases described in the present work are lamellar, with the possible exception of pure $(CL)_2Ca^{2+}$ (Cullis et al., 1978).

References

Chadwick, G. A. (1963–1964) *Prog. Mater. Sci. 12*, 97–182.

Cullis, P. R., Verkleij, A. J., & Ververgaert, P. H. J. Th. (1978) *Biochim. Biophys. Acta 513*, 11–20.

Eckwall, P. (1975) *Adv. Liq. Cryst. 1*, 1–142.

Galla, H. J., & Sackmann, E. (1975) *Biochim. Biophys. Acta 401*, 509–525.

Gent, M. P. N., & Ho, C. (1978) *Biochemistry 17*, 3023–3038.

Grant, C. W. M., Wu, S. H. W., & McConnell, H. M. (1974) *Biochim. Biophys. Acta 363*, 151–158.

Ise, N., & Okubo, T. (1980) *Acc. Chem. Res. 13*, 303–309.
Ladbrooke, B. D., & Chapman, D. (1969) *Chem. Phys. Lipids 3*, 304–356.
Lentz, B. R., Freire, E., & Biltonen, R. L. (1978) *Biochemistry 17*, 4475–4480.
Luna, E. J., & McConnell, H. M. (1977) *Biochim. Biophys. Acta 470*, 303–316.
Mabrey, S., Mateo, P. L., & Sturtevant, J. M. (1978) *Biochemistry 17*, 2464–2468.
Melchior, D. L., & Steim, J. M. (1979) *Prog. Surf. Membr. Sci. 13*, 211–296.
Miller, R. G. (1980) *Nature (London) 287*, 166–167.
Oldfield, E., & Chapman, D. (1972) *FEBS Lett. 23*, 285–297.
Owicki, J. C., & McConnell, H. M. (1980) *Biophys. J. 30*, 383–397.
Recktenwald, D., & McConnell, H. M. (1981) *Biochemistry 20*, 4505–4510.
Rubenstein, J. L. R., Smith, B. A., & McConnell, H. M. (1979) *Proc. Natl. Acad. Sci. U.S.A. 76*, 15–18.
Rubenstein, J. L. R., Owicki, J. C., & McConnell, H. M. (1980) *Biochemistry 19*, 569–573.
Shimshick, E. J., & McConnell, H. M. (1973) *Biochemistry 12*, 2351–2360.
Smith, L. M., Parce, J. W., Smith, B. A., & McConnell, H. M. (1979) *Proc. Natl. Acad. Sci. U.S.A. 76*, 4177–4179.
Verkleij, A. J., Mombers, C., Leunissen-Bijuelt, J., & Ververgaert, P. H. J. Th. (1979) *Nature (London) 279*, 162–163.
Wu, S. H. W., & McConnell, H. M. (1975) *Biochemistry 14*, 847–854.

Nucleotide Sequences of 5′ Termini of Adenovirus 2 Early Transforming Region E1a and E1b Messenger Ribonucleic Acids†

Shuichi Hashimoto,* William S. M. Wold, Karl H. Brackmann, and Maurice Green

ABSTRACT: The major 5′-terminal RNase T1 oligonucleotides derived from human adenovirus type 2 (Ad2) early regions E1a [map position (mp) 1.3–4.6] and E1b (mp 4.6–11.2) were characterized and sequenced. Poly(A+) polyribosomal RNA was isolated from Ad2-infected KB cell cultured 10 h in the presence of cycloheximide, the 5′-terminal m^7Gppp was removed, and the 5′-OH of the penultimate 2′-O-methylated nucleoside was labeled with [γ-^{32}P]ATP by using polynucleotide kinase. 5′-^{32}P-labeled poly(A+) RNA was hybridized to *Eco*RI-A (mp 0–58.5), *Hpa*I-E (mp 0–4.5), and *Hpa*I-C (mp 4.5–25) and to cloned fragments representing mp 0–4.5, 4.5–8, 8–10.7, 8–17, and 17–31.5. Fragment-specific mRNA was digested with RNase T1, the resulting oligonucleotides were resolved by two-dimensional paper electrophoresis–homochromatography, and the 5′-terminal methylated oligonucleotides were characterized by nuclease P1 digestion and two-dimensional thin-layer chromatography. Two major 5′-terminal RNase T1 oligonucleotides were obtained from *Eco*RI-A-specific mRNA; these were characterized by RNase T2 digestion and two-dimensional thin-layer chromatography and were sequenced by partial nuclease P1 digestion and electrophoresis–homochromatography. These two oligonucleotides were mapped to E1a and E1b, respectively, by analysis of E1a- and E1b-specific mRNA. Their sequences are as follows: E1a, m^7Gppp(m^6)A^{m}C$^{(m)}$UCUUGp; E1b, m^7Gppp(m^6)A^{m}C$^{(m)}$AUCUGp, in which the methylations shown in parentheses are partial. The E1a 5′-terminal oligonucleotide was found as a minor component of E1b mRNA, implying that mRNAs exist with both E1a and E1b sequences. Five other minor 5′-terminal oligonucleotides were observed in E1 mRNA, implying that transcription initiation is not always precise. Sequences corresponding to these two 5′ termini were found at nucleotide positions 498–504 (E1a) and 1699–1705 (E1b) in the Ad2 DNA sequence (T. Gingeras and R. Roberts, unpublished experiments), positions where the 5′-terminal region of E1a and E1b mRNAs has been mapped by nuclease gel analysis [Berk, A. J., & Sharp, P. A. (1978) *Cell (Cambridge, Mass.) 14*, 695–711] and electron microscopic visualization [Chow, L. T., Broker, T. R., & Lewis, J. (1979) *J. Mol. Biol. 134*, 265–303; Kitchingman, G. R., & Westphal, H. (1980) *J. Mol. Biol. 137*, 23–48]. E1a contains a TATA box at −24 to −31, a potential ribosome binding site at +22 to +32, and an ATG at +62 to +64. E1b contains a TATA box at −24 to −30, potential ribosome binding sites at +3 to +10 and +34 to +47, and ATGs at +13 to +15 and +317 to +319.

A major goal of eukaryotic molecular biologists is to understand the mechanism of transcription initiation, because this is central to the problem of gene regulation. The human adenovirus (Ads) are good models for such studies: many of the genes and their products have been well characterized, and much of the genome has been sequenced. As a prerequisite to understanding transcription initiation, it s necessary to localize, at the nucleotide level, exactly where transcription starts. Studies on the Ad2 major late transcription unit have indicated that transcription in vivo probably initiates at the cap site (Ziff & Evans, 1978). This also seems to occur in in vitro transcription systems (Weil et al., 1979; Manley et al., 1979). Therefore, the transcription initiation site of any transcription unit can be identified by sequencing the capped 5′ termini of RNA and then by locating the sequence within the DNA sequence.

In this paper, we have sequenced the major 5′ termini of mRNAs synthesized during early stages of Ad2 infection from Ad2 early region E1. E1 is located at map position (mp) 1.3–11.2, and E1 mRNAs are transcribed off the r the strand (Berk & Sharp, 1978; Chow et al., 1979; Kitchingman &

† From the Institute for Molecular Virology, St. Louis University Medical Center, St. Louis, Missouri 63110. *Received February 24, 1981.* This work was supported by U.S. Public Health Service Grant 9 R01 CA-29561. W.S.M.W. is the recipient of National Institutes of Health Research Career Development Award 1 K04 CA-00650. M.G. is the recipient of National Institutes of Health Research Career Award 5 K06 AI-04739.

0006-2960/81/0420-6640$01.25/0